Analysis on the cascade high power piezoelectric ultrasonic transducers

Shuyu Lin[*] and Jie Xu

Shaanxi key Laboratory of Ultrasonics, Shaanxi Normal University, 620 West Chang'an Street, China

Abstract. A new type of cascade sandwiched piezoelectric ultrasonic transducer is presented and studied. The cascade transducer is composed of two traditional longitudinally sandwiched piezoelectric transducers, which are connected together in series mechanically and in parallel electrically. Based on the analytical method, the electromechanical equivalent circuit of the cascade transducer is derived and the resonance/anti-resonance frequency equations are obtained. The impedance characteristics and the vibrational modes of the transducer are analyzed. By means of numerical method, the dependency of the resonance/anti-resonance frequency and the effective electromechanical coupling coefficient on the geometrical dimensions of the cascade transducer are studied and some interesting conclusions are obtained. Two prototypes of the cascade transducers are designed and made; the resonance/anti-resonance frequency is measured. It is shown that the analytical resonance/anti-resonance frequencies are in good agreement with the experimental results. It is expected that this kind of cascade transducer can be used in large power and high intensity ultrasonic applications, such as ultrasonic liquid processing, ultrasonic metal machining and ultrasonic welding and soldering.

Keywords: cascade piezoelectric transducer; longitudinal vibration; sandwiched transducer; effective electromechanical coupling coefficient

1. Introduction

Along with the development of ultrasonic technology, high power ultrasound are used in more and more applications in industry, electronics, medicine, environmental protection and many other fields, such as ultrasonic cleaning, ultrasonic welding and soldering, ultrasonic extraction, ultrasonic grinding, ultrasonic oil extraction, etc. In the field of high power ultrasonics, the longitudinally sandwiched piezoelectric ultrasonic transducer, which is also called Langevin composite piezoelectric transducer, is the leading device for the generation of high power ultrasound and has been widely used (Shoh 1970, Neppiras 1973, Minchenko 1969, Ranz-Guerra and Ruiz-Aguirre 1975, Michael 1988, Wevers and Lafaut 2005, Dubus and Debus 1991). It has the advantages of high mechanical strength, large output power and high electro-acoustic efficiency, simple and flexible structure. In order to improve the performance of the traditional longitudinally sandwiched piezoelectric ceramic transducer, related research work can alwaysbe found in some current publications (Athikom and Hari 1991, Arnold and Muhlen 2001, Arnold and Muhlen 2001, Hansen 1997, Arnold and Muhlen 2003, Parrini 2003, Iula and Vazquez 2002, Heikkola and Miettinen 2006, Heikkola and Laitinen 2005, Decastro and Johnson 2006, Lin 2004, Lin 2005).

For high power ultrasonic applications, such as ultrasonic cleaning, ultrasonic extraction and ultrasonic sonochemistry, high power and high ultrasonic intensity are

always expected for optimum ultrasonic processing effect. On the other hand, the ultrasonic radiation range of the ultrasonic transducer is also important for large volume of ultrasonic processing. In order to increase the ultrasonic power capacity of the ultrasonic transducer and the ultrasonic radiation range, new research work based on the traditional longitudinally sandwiched piezoelectric transducer is proposed and studied, and some new structure and design are given (Gachagan and McNab 2004, Fu and Xian 2012, Peshkovsky and Peshkovsky 2007, Dahlem and Reisse 1999, Abramov 1998, Walter 1993, Hu and Lin 2014, Lin and Fu 2013, Lin and Fu 2013, Zhang and Lin 2013, Lin and Xu 2011).

In this paper, based on the traditional longitudinally sandwiched piezoelectric transducer, a new type of cascade high power piezoelectric transducer is proposed. It is a combination of two or more sandwiched piezoelectric transducers, wherein each transducer is a longitudinal vibrator of half a wavelength with thin electrodes, which are connected together electrically in parallel and mechanically in series. These transducers are simultaneously excited by the same electric signal. Compared with the traditional longitudinally sandwiched piezoelectric transducer, the cascade transducer has the following advantages. First, the input electric power can be further increased, and therefore, its ultrasonic intensity can also be increased. Second, the cascade transducer is similar to the traditional sandwiched piezoelectric transducer with a thick electrode. In this case, the heat conductive performance of the transducer can be further improved, and therefore, the efficiency and the output power can be increased.

In the following analysis, the electromechanical equivalent circuit of the cascade transducer is first derived.

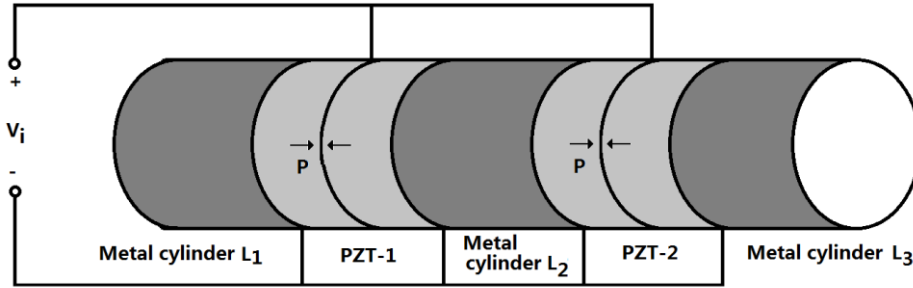∗Corresponding author, Professor
 E-mail: sylin@snnu.edu.cn

Fig. 1 A cascade longitudinally sandwiched piezoelectric transducer

Then the resonance/anti-resonance frequency equations are obtained. Finally, the relationship between the electromechanical characteristics and the geometrical dimensions is analyzed, and some optimization design rules for this kind of cascade transducer are given.

2. Theoretical analysis of the cascade sandwiched piezoelectric ultrasonic transducer

The cascade sandwiched transducer is shown in Fig. 1. It consists of two traditional longitudinally sandwiched piezoelectric transducers. The two longitudinally sandwiched piezoelectric transducers are connected together mechanically in series, and electrically in parallel. In the cascade transducer, there are two groups of piezoelectric ceramic stacks and three metal cylinders, which are clamped together by a central high strength metal bolt. The metal bolt supply appropriate pre-stressing force for clamping the components of the cascade transducer. In Fig.1, the arrow P represents the polarization direction of the piezoelectric ceramic element. When the external electric signal from an ultrasonic generator is applied to the piezoelectric ceramic stacks, the cascade transducer will produce longitudinal vibration in the longitudinal direction because of the inverse piezoelectric effect. When the frequency of the exciting signal is equal to the resonance frequency of the transducer, the cascade transducer will resonate at a definite vibrational mode. In this case, the longitudinal vibration of the transducer reaches a maximum value. According to the traditional one-dimensional analytical theory, it is required that the cross sectional dimensions should be much less than its longitudinal dimension.

On the other hand, from Fig. 1, it can be seen that the cascade longitudinally sandwiched piezoelectric transducer can also be considered as a traditional longitudinally sandwiched piezoelectric transducer with a thick electrode of length L_2. In this case, the heat conductive performance of the transducer can be improved by the insertion of the thick metal electrode and therefore, the electric power and electroacoustic efficiency of the transducer can be effectively increased.
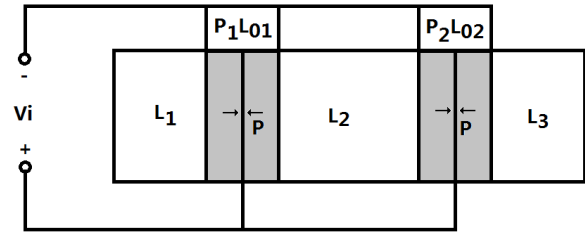

Fig. 2 Geometrical sketch of a cascade longitudinally sandwiched piezoelectric transducer

The geometrical sketch of the cascade transducer is shown in Fig. 2. In the figure, the length of the three metal cylinders are L_1, L_2 and L_3. The length for the two piezoelectric ceramic stacks is $p_1 L_{01}$ and $p_2 L_{02}$, p_1 and p_2 are the number of the piezoelectric elements in the piezoelectric stacks. The radius of the three metal cylinders and the piezoelectric ceramic stacks are R_1, R_2, R_3 and R_{01}, R_{02} respectively. For simplicity in the following analysis, it is assumed that $R_1 = R_2 = R_3 = R_{01} = R_{02}$.

Based on the electromechanical equivalent circuit of the longitudinally sandwiched composite piezoelectric transducer (Lin 2005, Lin 2009, Lin and Xu 2008), when the mechanical and the dielectric losses in the transducer are not considered, the equivalent circuit of the cascade transducer as shown in Fig. 1 can be obtained as shown in Fig. 3. It should be pointed out that the equivalent circuit as shown in Fig. 3 is based on one-dimensional longitudinally vibrational theory. It is assumed that the lateral dimension should be much less than the longitudinal dimension of the transducer. Generally speaking, when the lateral dimension is less than a quarter of the longitudinally vibrational wavelength, one-dimensional longitudinally vibrational theory is basically applicable to the analysis of the transducer. In the figure, parts 1, 3 and 5 represent the three metal cylinders, and parts 2 and 4 represent the two piezoelectric ceramic stacks, respectively. V_i is the input voltage of the transducer. Z_{L1} and Z_{L2} are the load mechanical impedances of the transducer. C_1, C_2 and n_1, n_2 are the clamped capacitance and electro-mechanical
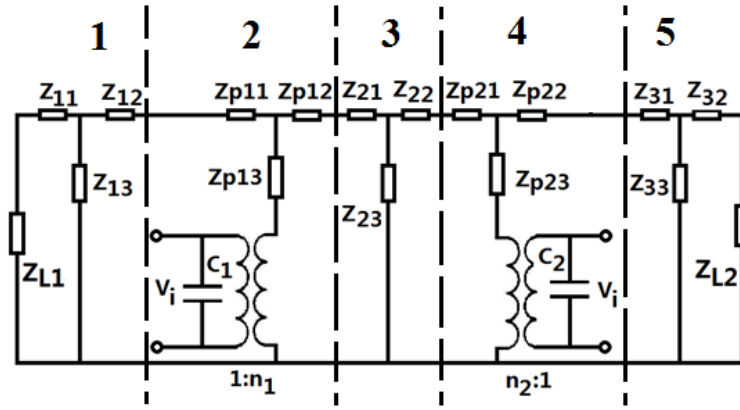
Fig. 3 Electro-mechanical equivalent circuit of a cascade sandwiched piezoelectric transducer

conversion coefficient of the piezoelectric transducers.

Their expressions are as follows

$$C_1 = p_1\varepsilon_{33}^T(1-K_{33}^2)S_{01}/L_{01}, \quad C_2 = p_2\varepsilon_{33}^T(1-K_{33}^2)S_{02}/L_{02} \quad (1)$$

$$n_1 = d_{33}S_{01}/(s_{33}^E L_{01}), \quad n_2 = d_{33}S_{02}/(s_{33}^E L_{02}) \quad (2)$$

Where, S_{01} and S_{02} are the cross sectional areas of the two piezoelectric ceramic stacks. $S_{01} = S_{02} = \pi R_{01}^2$, ε_{33}^T, K_{33}, d_{33} and s_{33}^E are the dielectric constant, the electromechanical coupling coefficient, the piezoelectric constant and the elastic compliance constant of the piezoelectric material. In Fig. 3, the expressions for the series and parallel impedances in the circuit are as follows

$$Z_{11} = Z_{12} = jZ_1\tan(\frac{k_1L_1}{2}), \quad Z_{13} = \frac{Z_1}{j\sin(k_1L_1)} \quad (3)$$

$$Z_{21} = Z_{22} = jZ_2\tan(\frac{k_2L_2}{2}), \quad Z_{23} = \frac{Z_2}{j\sin(k_2L_2)} \quad (4)$$

$$Z_{31} = Z_{32} = jZ_3\tan(\frac{k_3L_3}{2}), \quad Z_{33} = \frac{Z_3}{j\sin(k_3L_3)} \quad (5)$$

$$Z_{P11} = Z_{P12} = jZ_{01}\tan(\rho_1 k_0 L_{01}/2), \quad Z_{P13} = \frac{Z_{01}}{j\sin(\rho_1 k_0 L_{01})} \quad (6)$$

$$Z_{P21} = Z_{P22} = jZ_{02}\tan(\rho_2 k_0 L_{02}/2), \quad Z_{P23} = \frac{Z_{02}}{j\sin(\rho_2 k_0 L_{02})} \quad (7)$$
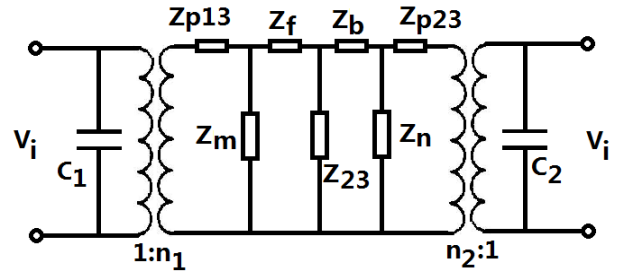

Fig. 4 Transformed electromechanical equivalent circuit of a cascade transducer

In these equations, $Z_1 = \rho_1 c_1 S_1$, $k_1 = \omega/c_1$, $c_1 = (E_1/\rho_1)^{1/2}$, $S_1 = \pi R_1^2$, $Z_2 = \rho_2 c_2 S_2$, $k_2 = \omega/c_2$, $c_2 = (E_2/\rho_2)^{1/2}$, $S_2 = \pi R_2^2$, $Z_3 = R_3 c_3 S_3$, $k_3 = \omega/c_3$, $c_3 = (E_3/\rho_3)^{1/2}$, $S_3 = \pi R_3^2$. $Z_{01} = \rho_0 c_0 S_{01}$, $Z_{02} = \rho_0 c_0 S_{02}$, $k_0 = \omega/c_0$, $c_0 = [1/(s_{33}^E\rho_0)]^{1/2}$. ρ_1, E_1, ρ_2, E_2 and ρ_3, E_3 are density and Young's modulus of the three metal cylinders; c_1, c_2, c_3 and c_0 are sound speed of longitudinal vibration in the metal cylinders and the piezoelectric stacks.

Based on the equivalent circuit of the cascade transducer, after some circuit transformations, Fig. 3 can be transformed to Fig. 4.

In Fig. 4, the expressions for the circuit impedances are as follows

$$Z_f = Z_{P12} + Z_{21} \quad (8)$$
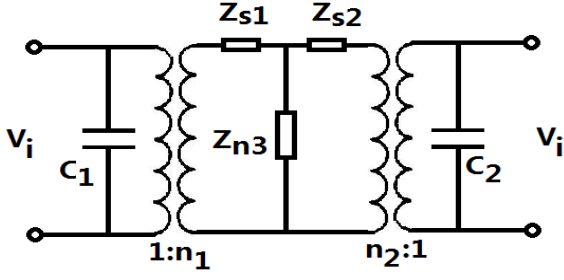
$$Z_b = Z_{P21} + Z_{22} \quad (9)$$

Fig. 5 Simplified equivalent circuit of the cascade transducer

$$Z_m = Z_{P11} + Z_{12} + \frac{Z_{13}(Z_{11} + Z_{L1})}{Z_{13} + Z_{11} + Z_{L1}} \tag{10}$$

$$Z_n = Z_{P22} + Z_{31} + \frac{Z_{33}(Z_{32} + Z_{L2})}{Z_{33} + Z_{32} + Z_{L2}} \tag{11}$$

From Fig. 4, after two times of circuit transformations of star-triangle-star circuit, a simplified equivalent circuit model can be further obtained as shown in Fig. 5. In the figure, the expressions for the circuit impedances are as follows,

$$Z_{s1} = Z_{P13} + Z_{n1} \tag{12}$$

$$Z_{s2} = Z_{P23} + Z_{n2} \tag{13}$$

$$Z_{n1} = \frac{Z_{t1} Z_{m1}}{Z_{t1} + Z_{m1} + Z_{m2}} \tag{14}$$

$$Z_{n2} = \frac{Z_{t1} Z_{m2}}{Z_{t1} + Z_{m1} + Z_{m2}} \tag{15}$$

$$Z_{n3} = \frac{Z_{m1} Z_{m2}}{Z_{t1} + Z_{m1} + Z_{m2}} \tag{16}$$

$$Z_{m1} = \frac{Z_{t2} Z_m}{Z_{t2} + Z_m} \tag{17}$$

$$Z_{m2} = \frac{Z_{t3} Z_n}{Z_{t3} + Z_n} \tag{18}$$

$$Z_{t1} = \frac{Z_f Z_b + Z_f Z_{23} + Z_b Z_{23}}{Z_{23}} \tag{19}$$

$$Z_{t2} = \frac{Z_f Z_b + Z_f Z_{23} + Z_b Z_{23}}{Z_b} \tag{20}$$

$$Z_{t3} = \frac{Z_f Z_b + Z_f Z_{23} + Z_b Z_{23}}{Z_f} \tag{21}$$

From Fig. 5, the input electric impedance Z_i of the cascade transducer can be obtained as the following equation

$$Z_i = \frac{Z_{i1} Z_{i2}}{Z_{i1} + Z_{i2}} \tag{22}$$

Where, Z_{i1} and Z_{i2} are the input electric impedances of the two piezoelectric stacks of the transducer. Their expressions are

$$Z_{i1} = \frac{Z_{c1} Z_{rm1}}{n_1^2 Z_{c1} + Z_{rm1}} \tag{23}$$

$$Z_{i2} = \frac{Z_{c2} Z_{rm2}}{n_2^2 Z_{c2} + Z_{rm2}} \tag{24}$$

$$Z_{rm1} = \frac{Z_{n3}^2 - (Z_{s1} + Z_{n3})(Z_{s2} + Z_{n3})}{(n_2/n_1) Z_{n3} - (Z_{s2} + Z_{n3})} \tag{25}$$

$$Z_{rm2} = \frac{Z_{n3}[Z_{n3}^2 - (Z_{s1} + Z_{n3})(Z_{s2} + Z_{n3})]}{(n_1/n_2)[Z_{n3}^2 - (Z_{s1} + Z_{n3})(Z_{s2} + Z_{n3})] - Z_{n3}(Z_{s1} + Z_{n3}) + (n_1/n_2)(Z_{s1} + Z_{n3})(Z_{s2} + Z_{n3})} \tag{26}$$

$$Z_{c1} = \frac{1}{j\omega C_1} \tag{27}$$

$$Z_{c2} = \frac{1}{j\omega C_2} \tag{28}$$

Where, Z_{c1} and Z_{c2} are the impedances of the clamped capacitances, Z_{rm1} and Z_{rm2} are the mechanical impedances for the two piezoelectric ceramic stacks. From Eq. (22), when the load mechanical impedances of the transducer are neglected, which means that the mechanical terminals of the transducer are short circuited, the frequency response of the input electric impedance of a cascade transducer can be obtained as shown in Fig. 6. In the
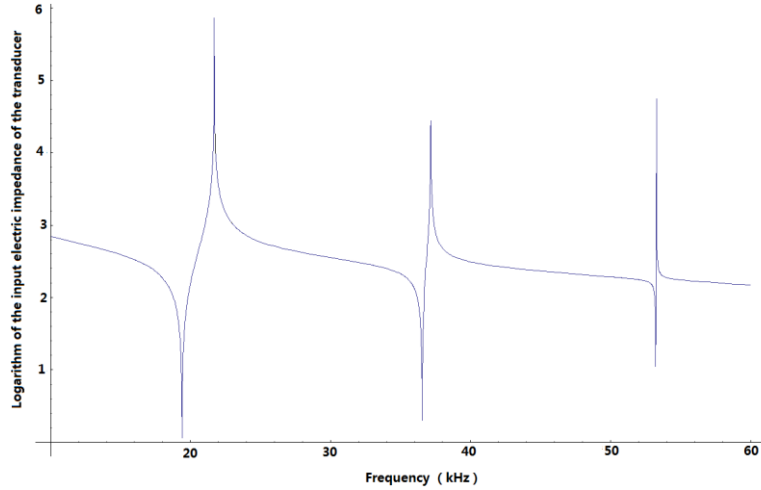
Fig. 6 Frequency response of the input electric impedance for a cascade transducer

numerical calculation, the material for the metal cylinders is aluminium alloy, its standard material parameters are used and as follows: $\rho_1 = \rho_2 = \rho_3 = 2790 kg / m^3$, $E_1=E_2=E_3=6.85\times10^{10}\text{N/m}^2$. The piezoelectric material is an equivalent of PZT-4, the related material parameters are: $\rho_{01}=\rho_{02}=7500\text{kg/m}^3$, $s_{33}^E=15.5\times10^{-12}\text{m}^2\text{/N}$, $K_{33}=0.7$, $d_{33}=496\times10^{-12}\text{C/N}$, $\varepsilon_0=8.8542\times10^{-12}\text{F/m}$, $\varepsilon_{33}^T/\varepsilon_0=1300$.

The geometrical dimensions for the cascade transducer are as follows: L_1=0.03 m, L_2=0.02 m, L_3=0.05 m, $L_{01}=L_{02}$=0.005 m, $R_1= R_2= R_3 = R_{01} = R_{02} = 0.0195$ m, $p_1=p_2=2$.

In Fig. 6, the y-axis is the logarithm of the input electric impedance of the cascade transducer, the x-axis represents the frequency. It can be seen that since the mechanical loss, the dielectric loss and the load mechanical impedance are not considered, the minimum value of the input electric impedance of the transducer is nearly equal to zero, and the maximum input electric impedance of the transducer tends to the infinity. On the other hand, from the frequency response curve of the transducer, it can be seen that the transducer has many vibrational modes. At different vibrational modes, the vibrational characteristics are different. In practical applications, these vibrational modes can be used for different applications.

Based on the frequency response curve and the definition of the resonance/anti-resonance frequency of the transducer, the design equations for the resonance/anti-resonance frequency of the transducer can be obtained as follows

$$Z_i = \frac{Z_{i1}Z_{i2}}{Z_{i1} + Z_{i2}} = 0 \tag{29}$$

$$Z_i = \frac{Z_{i1}Z_{i2}}{Z_{i1} + Z_{i2}} \rightarrow \infty \tag{30}$$

Eqs. (29) and (30) are the resonance frequency and the anti-resonance frequency equations, respectively. When the material parameters and the geometrical dimensions of the transducer are defined, the resonance frequency f_r and the anti-resonance frequency f_a at different vibrational modes can be obtained. Based on the resonance frequency and the anti-resonance frequency, the effective electromechanical coupling coefficient K_{effc} of the transducer can be calculated according to the following equation

$$K_{effc} = \sqrt{1 - (f_r / f_a)^2} \tag{31}$$

3. Theoretical relationship between the resonance/anti-resonance frequency and the effective electromechanical coupling coefficient with the geometrical dimension

In order to optimize the electromechanical characteristics of the cascade transducer, the dependency of the resonance/anti-resonance frequency and the effective electromechanical coupling coefficient on the geometrical dimension of the transducer is theoretically analysed. In this section, the resonance/anti-resonance frequency of the transducer is first found from the frequency Eqs. (29) and (30) by numerical method. Then the effective electromechanical coupling coefficient is calculated by using Eq. (31). In the numerical calculation, the material for the metal cylinders is aluminium alloy; the piezoelectric material is an equivalent of PZT-4. The standard material parameters are used and the same as those in the above section. The geometrical dimensions for the cascade transducer are as follows: L_1=0.06m, L_2+L_3=0.18m, $L_{01}=L_{02}$=0.005m, $R_1= R_2= R_3= R_0 = R_0 = $, $p_1=p_2=2$. In the numerical simulation, the total length of the transducer is kept unchanged. When the length L_2 of the middle metal cylinder is changed, the theoretical
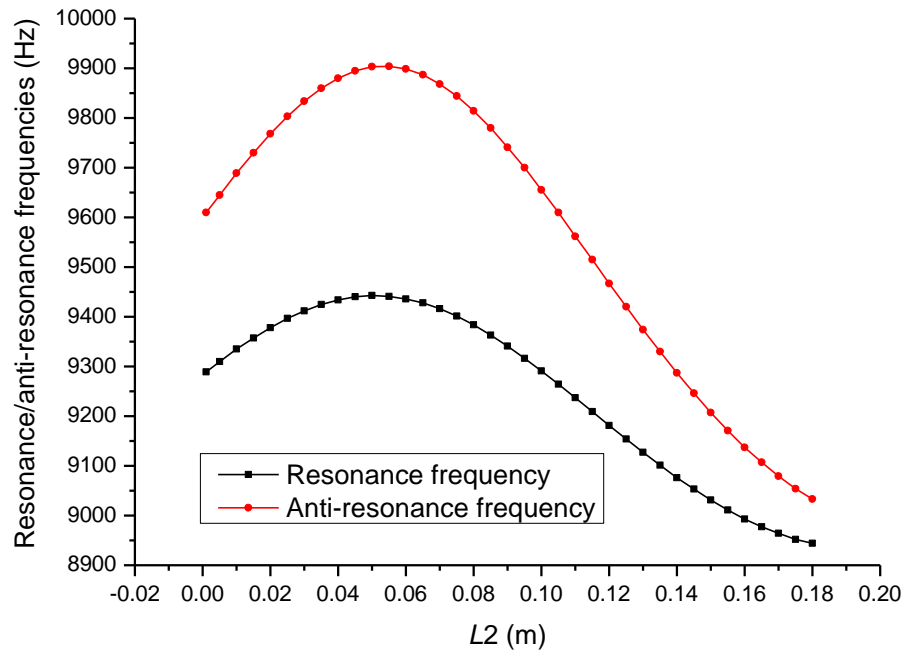
Fig. 7 Theoretical relationship between the resonance/anti-resonance frequency and length L_2 for the first vibrational mode
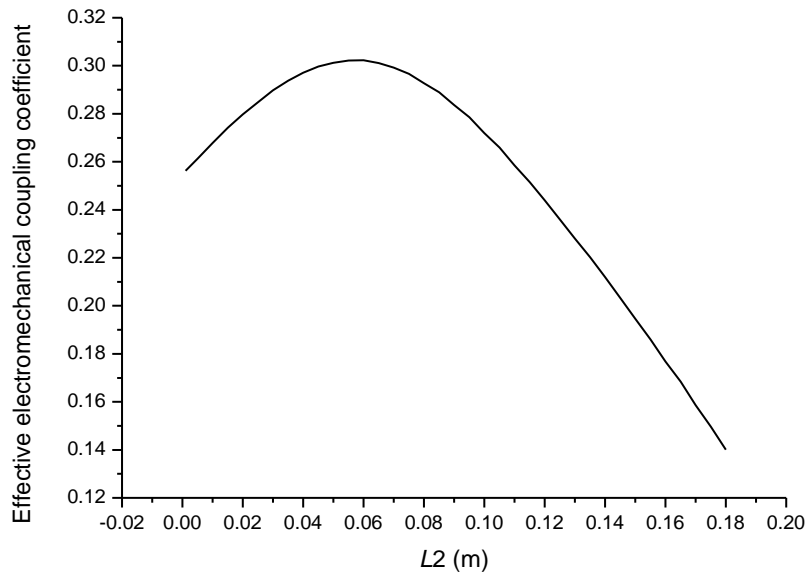

Fig. 8 Dependency of the effective electromechanical coupling coefficient on length L_2 for the first vibrational mode

relationship between the resonance/anti-resonance frequencies, the effective electromechanical coupling coefficient and the length L_2 are shown in Figs. 7-10.

From Figs. 1 and 2, it can be seen that the variation of the length L_2 means the variation of the distance between the two piezoelectric ceramic stacks in the transducer.

From Figs. 7 and 8, it can be seen that for the first vibrational mode, when the length L_2 is increased, which means that the second piezoelectric stack becomes far away from the first piezoelectric stack, the resonance/anti-resonance frequencies and the effective electromechanical coupling coefficient are generally decreased.
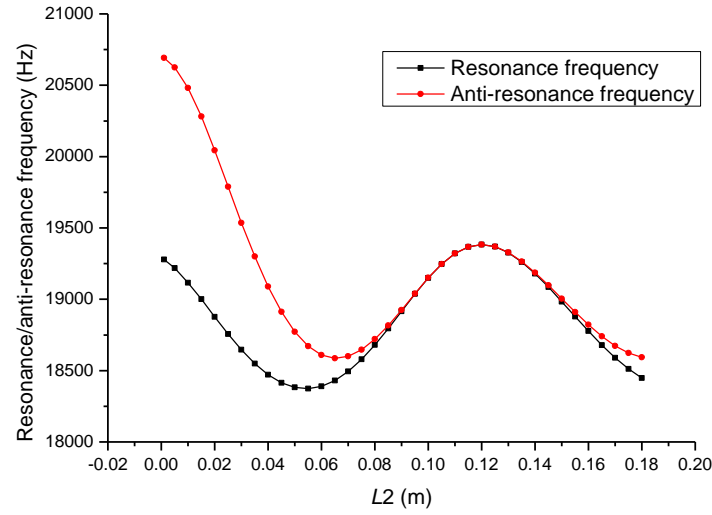
Fig. 9 Theoretical relationship between the resonance/anti-resonance frequency and length L_2 for the second vibrational mode
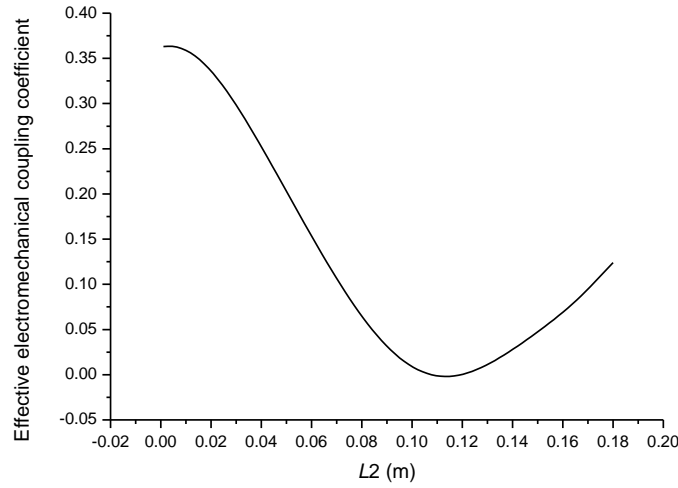

Fig. 10 Dependency of the effective electromechanical coupling coefficient on length L_2 for the second vibrational mode

However, corresponding to a definite length L_2, there is a maximum value for the resonance/anti-resonance frequencies and the effective electromechanical coupling coefficient, and this conclusion can be used for the optimization of the cascade transducer. For the second vibrational mode, it can be seen from Figs. 9 and 10 that the resonance/anti-resonance frequencies are changed periodically with the length L_2. Corresponding to a definite length L_2, the effective electromechanical coupling coefficient has a minimum value, this should be avoided in the design of the transducer.

4. Experiments

In order to verify the analytical design theory for the cascade transducer, some prototypes of the cascade transducers are designed and manufactured. The geometrical dimensions of the prototypes of transducers are listed in Table 1. The material for the metal cylinders in the transducers is aluminum alloy and the piezoelectric ceramic material is an equivalent of PZT-4. The standard material parameters are used which are the same as those in the above analysis. The resonance/anti-resonance frequencies are measured by using 6500B Precision Impedance.
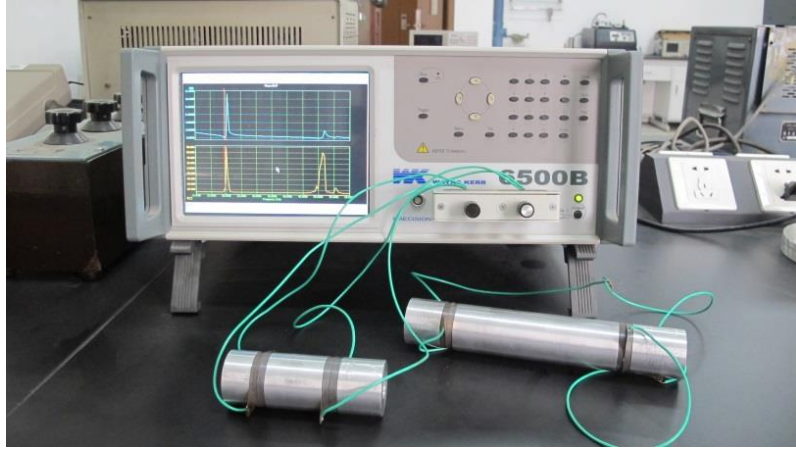
Fig. 11 Experimental set-up for the measurement of the resonance/anti-resonance frequency

Table 1 Geometrical dimensions of the cascade piezoelectric transducers

No.	$L_1(mm)$	$L_2(mm)$	$L_3(mm)$	$L_{01}(mm)$	$L_{02}(mm)$	p_1	p_2	$R_1=R_2=R_3(mm)$	$R_{01}=R_{02}(mm)$
1	30.0	40.0	20.0	5.0	5.0	2	2	19.5	19.0
2	30.0	130.0	40.0	5.0	5.0	2	2	19.5	19.0

Analyzer made by Wayne Kerr Electronics of West Sussex in UK as shown in Fig. 11. The numerically calculated and measured curves of the input electric impedance versus the frequency for a cascade transducer are shown in Fig. 12. In the figure, the longitudinal axis represents the logarithm value of the input electric impedance of the transducer. Fig. 12(a) is the numerically calculated curve based on Eq. (22); Fig. 12(b) is the experimentally measured result. From Fig. 12, it can be seen that the numerically calculated logarithm value of the input electric impedance is different from the experimentally measured logarithm value of the input electric impedance. The reason is that in the theoretical analysis, all the losses, including the mechanical loss in the material, the dielectric loss in the piezoelectric material and the contacting mechanical loss in the transducer are all not considered, while in the real transducer, all these losses are present. On the other hand, it can be seen that the resonance/anti-resonance frequencies which correspond to the minimum and maximum value of the input electric impedance in the curves are almost the same for the numerically calculated and measured results. It is therefore concluded that the effect of the losses on the resonance/anti-resonance frequencies of the transducer is negligible. From the measured curves of the input electric impedance versus the frequency, the resonance/anti-resonance frequencies of the transducers can be obtained. The analytical and experimental resonance/anti-resonance frequencies of the transducers are listed in Tables 2 and 3. In these tables, f_r and f_a are the analytical resonance/anti-resonance frequencies; f_{mr} and f_{ma} are the measured results.

$$\Delta_1 = |f_r - f_{mr}|/f_{mr}, \quad \Delta_2 = |f_a - f_{ma}|/f_{ma}.$$

Table 2 Analytical and experimental resonance/anti-resonance frequencies of the transducers at the first vibrational mode

No.	f_r(Hz)	f_{mr}(Hz)	Δ_1(%)	f_a(Hz)	f_{ma}(Hz)	Δ_2(%)
1	19786	19709	0.39	21399	20555	4.1
2	10202	10078	1.23	10414	10374	0.39

Table 3 Analytical and experimental resonance/anti-resonance frequencies of the transducers at the second vibrational mode

No.	f_r(Hz)	f_{mr}(Hz)	Δ_1(%)	f_a(Hz)	f_{ma}(Hz)	Δ_2(%)
1	58611	50719	15.6	60926	52159	16.8
2	33044	32394	2.0	35459	34341	3.26

From the above results, it can be seen that for the first vibrational mode of the transducer, the experimental resonance/anti-resonance frequencies are in good agreement with the theoretical results. For the second vibrational mode, the error between the theoretical and the experimental resonance/anti-resonance frequencies is comparatively large. The reason may be explained as follows. First, the standard material parameters are more or less different from the real material parameters. Second, the mechanical loss and the dielectric loss are not considered in the theoretical analysis. Third, in the theoretical analysis, one-dimensional theory is assumed.

(A). Numerically calculated curve
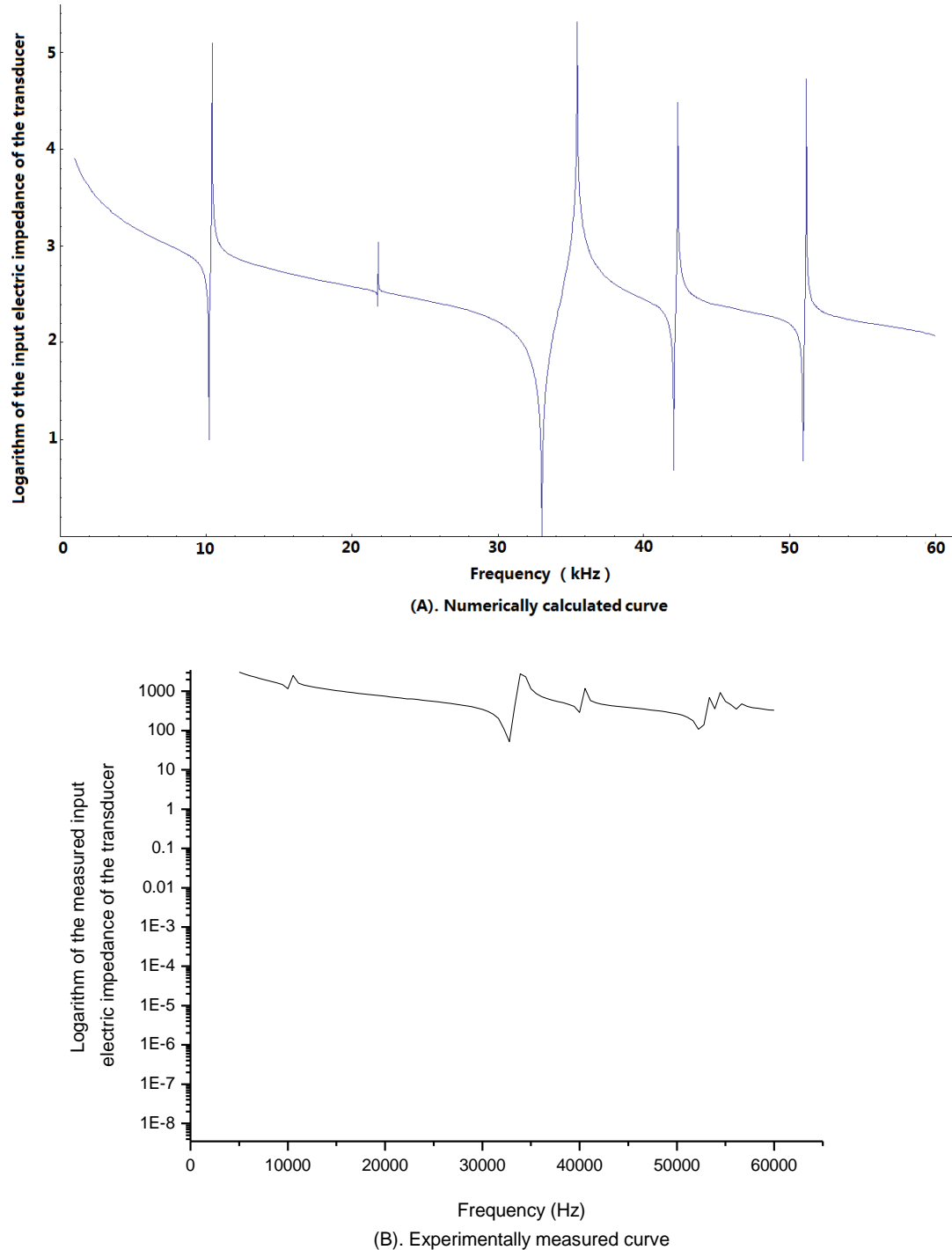

(B). Experimentally measured curve

Fig. 12 Analytic and measured curves of the input electric impedance versus the frequency for a   cascade piezoelectric transducer

However, for the real transducers, the lateral dimension is not much less than the longitudinal length of the transducer. This is especially obvious for the second vibrational mode of the transducer.

Fourth, in the theoretical analysis, the prestressing bolt is not considered. In practical situations, the transducer is clamped by a central prestressing metal bolt.

Table 4 lists the analytical and experimental effective electromechanical coupling coefficient of the transducers.

In the table, K_{effc} is the theoretical effective electromechanical coupling coefficient; K_{effc-m} is the experimental effective electromechanical coupling coefficient. It can be seen that the theoretical and experimental effective electromechanical coupling coefficients are basically in agreement with each other.

Table 4 Analytical and experimental effective electromechanical coupling coefficient of the transducers

No.	First mode		Second mode	
	K_{effc}	$K_{effc\text{-}m}$	K_{effc}	$K_{effc\text{-}m}$
1	0.381	0.284	0.273	0.233
2	0.201	0.237	0.363	0.332

5. Conclusions

A new type of cascade sandwiched piezoelectric transducer is studied. The resonance/anti-resonance frequency equations are obtained. The dependency of the resonance/anti-resonance frequency and the effective electromechanical coupling coefficient on the geometrical dimensions is analyzed. To sum up the above analysis, the following conclusions can be drawn out.

- The cascade transducer can be operated on different vibrational modes depending on different requirements for the frequency and characteristics.

- For the first vibrational mode, when the length of the middle metal cylinder is changed, the resonance/anti-resonance frequency and the effective electromechanical coupling coefficient have maximum values.

- For the second vibrational mode, when the length of the middle metal cylinder is changed, the resonance/anti-resonance frequency and the effective electromechanical coupling coefficient have minimum values.

- One-dimensional longitudinal vibrational theory is used in the theoretical analysis and it is assumed that the lateral dimension should be much less than the longitudinal dimension of the transducer.

- The effect of the mechanical loss, the dielectric losses and the load mechanical impedance on the characteristics of the cascade transducer will be studied in future research.

Acknowledgments

References

Abramov, O.V. (1998), *High-Intensity Ultrasonics: Theory and Industrial Applications*, Gorden and Breach Science Publishers, Amsterdam, The Netherlands.

Arnold, F.J. and Muhlen, S.S. (2003), "The influence of the thickness of non-piezoelectric pieces on pre-stressed piezotransducers", *Ultrasonics*, **41**, 191-196.

Athikom, B., Hari, K. and P.and Robert, D.F. (1991), "Optimizing the performance of piezoelectric drivers that use stepped horns", *J. Acoust. Soc. Am.*, **90**, 1223-1229.

Arnold, F.J. and Muhlen, S.S. (2001), "The mechanical pre-stressing in ultrasonic piezotransducers", *Ultrasonics*, **39**, 7-11.

Arnold, F.J. and Muhlen, S.S. (2001), "The resonance frequencies on mechanically pre-stressed ultrasonic Piezotransducers", *Ultrasonics*, **39**, 1-5.

Dahlem, O., Reisse, J. and Halloin, V. (1999), "The radially vibrating horn: A scaling-up possibility for sonochemical reactions", *Chem. Eng. Sci.*, **54**, 2829-2838.

Dubus, B. and Debus, J.C. (1991), "Analysis of mechanical limitations of high power piezoelectric transducers using finite element modeling", *Ultrasonics*, **29**, 201-207.

Decastro, A.E. and Johnson, B.R. (2006), *High power ultrasonic transducer with broadband frequency characteristics at all overtones and harmonics*, United States. US Patent, **7019439, B2**.

Fu, Z.Q., Xian, X.J. and Lin, S.Y. (2012), "Investigations of the barbell ultrasonic transducer operated in the full-wave vibrational mode", *Ultrasonics*, **52**, 578-586.

Gachagan, A., McNab, A., Blindt, R., Patrick, M. and Marriott, C. (2004), "A high power ultrasonic array based test cell", *Ultrasonics,* **42**, 57-68.

Hansen, H.H. (1997), "Optimal design of an ultrasonic transducer", *Struct. Optim.*, **14**, 150-157.

Heikkola, E., Miettinen, K. and Nieminen, P. (2006), "Multiobjective optimization of an ultrasonic transducer using NIMBUS", *Ultrasonics*, **44**, 368-380.

Heikkola, E. and Laitinen, M. (2005), "Model-based optimization of ultrasonic transducers", *Ultrasonics Sonochemistry*, **12**, 53-57.

Hu, J., Lin, S.Y. and Zhang, X.L. (2014), "Radially Sandwiched composite transducers composed of the radially polarized piezoelectric ceramic circular ring and metal rings", *Acta Acustica United with Acustica*, **100**, 418-426.

Iula, A., Vazquez, F., Pappalardo, M. and Gallego, J.A. (2002), "Finite element three-dimensional analysis of the vibrational behavior of the Langevin-type transducer", *Ultrasonics*, **40**, 513-517.

Lin, S.Y. (2004), "Optimization of the performance of the sandwich piezoelectric ultrasonic transducer", *J. Acoust. Soc. Am.*, **115**, 182-186.

Lin, S.Y. (2005), "Analysis of the sandwich piezoelectric ultrasonic transducer in coupled vibration", *J. Acoust. Soc. Am.*, **117**, 653-661.

Lin, S.Y., Fu, Z.Q. and Zhang, X.L. (2013), "Radial vibration and ultrasonic field of along tubular ultrasonic radiator", *Ultrasonics Sonochemistry*, **20**, 1161-1167.

Lin, S.Y., Fu, Z.Q., Wang, Y. and Hu, J. (2013), "Radially sandwiched cylindrical piezoelectric transducer", *Smart Mater. Struct.*, **22**, 015005 (10pp).

Lin, S.Y., Xu, L. and Hu, W.X. (2011), "A new type of high power composite ultrasonic transducer", *J. Sound Vib.*, **330**, 1419-1431.

Lin, S.Y. (2005), "Load characteristics of high power sandwich piezoelectric ultrasonic transducers", *Ultrasonics*, **43**, 365-373.

Lin,S.Y.(2009), "Analysis of multifrequency Langevin composite ultrasonic transducers", *IEEE T. UFFC*, **56**, 1990-1998.

Lin, S.Y. and Xu, C.L. (2008), "Analysis of the sandwich ultrasonic transducer with two sets of piezoelectric elements", *Smart Mater. Struct.*, **17**, 065008 (8pp).

Michael, P.J. (1988), "Velocity control and the mechanical impedance of single degree of freedom electromechanical vibrators", *J. Acoust. Soc. Am.*, **84**, 1994-2001.

Minchenko, H. (1969), "High-power piezoelectric transducer design", *IEEE T. Sonics Ultrasonics*, **16**, 126-136.

Neppiras, E.A.(1973), "The pre-stressed piezoelectric sandwich transducer", *Proceedings of the Ultrasonics International Confenence* .

Parrini, L. (2003), "New technology for the design of advanced ultrasonic transducers for high-power applications", *Ultrasonics,* **41**, 261-269.

Peshkovsky, S.L. and Peshkovsky, A.S. (2007), "Matching a transducer to water at cavitation: Acoustic horn design principles", *Ultrasonics Sonochemistry*, **14**, 314-322.

Ranz-Guerra, C. and Ruiz-Aguirre, R.D. (1975), "Composite sandwich transducers with quarter-wavelength radiating layers", *J. Acoust. Soc. Am.*, **58**, 494-498.

Shoh, A. (1970), Sonic transducer, US Patent**. No. 3524085**.

Wevers, M., Lafaut, J.P., Baert, L. and Chilibon, I. (2005), "Low-frequency ultrasonic piezoceramic sandwich transducer", *Sensor. Actuat. – A*, **122**, 284-289.

Walter, *et al*. (1993), *Ultrasonic Transducer*, United States Patent. **5200666**.

Zhang, X.L., Lin, S.Y., Fu, Z.Q. and Wang, Y. (2013), "Coupled vibration analysis for a composite cylindrical piezoelectric ultrasonic transducer", *Acta Acustica United with Acustica*, **99**, 201-207.

CY